JOURNAL of QASSIM UNIVERSITY FOR SCIENCE
Vol. 1, Issue 1, pp 14-26 (October 2022)
JQUS

Effect of Thickness on The Optical Properties of CdS/CdTe Thin Films

Aiyeshah Alhodaib[1, *] and Norah Alhagass [2]

[1] Department of Physics, College of Science, Qassim University, Buraydah 51452, Saudi Arabia; ahdieb@qu.edu.sa

[2] Department of Physics, Collage of Science and Arts in Unizah, Qassim University, Unizah, Saudi Arabia

Correspondence author: ahdieb@qu.edu.sa

Abstract

In This paper, we present the preparation of CdTe/CdS hetero structure thin films, in addition to study of the physical properties for the prepared thin films. The effect of changing the thickness on the structural properties and the lattice constants have been investigated. The change in the optical properties and the optical constants were also studied.

Key Words: Thin films, solar cells, CdS/CdTe, Structural Properties, Optical Properties.

1. Introduction

The use of solar energy has progressively developed over the last decades, out of this relatively there is a need to consider and utilize alternative renewable energy sources that are eco-friendly and cost-effective materials with improvement in their efficiency [1]. In addition, the rapid and successive technological growth in the discovery of new semiconductor materials are suitable for the manufacturing of optoelectronic and solar cells that have many important effects on the technical expansion of modern societies [2]. The development of optoelectronic and photonic devices also contributes to increasing the efficiency of solar cells, which are widely used in converting solar energy into electrical energy as a source of clean energy. Recently, development of preparing and

studying the photoelectron and photonic devices in the nanometer range, in particular second generation solar cells which comprises different semiconductor layers of either absorber or active materials showed distinctive properties that were not known before [3].

Group II-VI semiconductor based on Cadmium Telluride (CdTe) has become suitable materials with low-cost and high efficiency of around ~22% or higher [4,5]. These materials are characterized by their direct bandgaps and large energy gaps in the range from 1eV to 3eV, this energy range is within the visible light area of the spectrum which has multiple technological applications in our daily life, such as solar energy converters (photovoltaic converter). In addition, Cadmium Sulfide (CdS) has been known as a window or buffer layer material for fabricated CdTe solar cell [6].

Previous studies reported that CdTe thin film solar cell having the higher efficiency in the range of 18-24%, the CdTe thin films solar cells have been used as a decent candidate for large scale manufacturing [7-12]. Different techniques have been used to produce a thin film Photovoltaic solar cells such as sputtering [6,13], Chemical Vapor Deposition (MOCVD) [7,14], Closed Spaced Sublimation (CSS) [8,15], thermal evaporation [9,16-17] and Molecular Beam Epitaxy (MBE) [10,18-19]. Close spaced sublimation (CSS) and thermal evaporation techniques can produce a homogeneous thin film [20].

In this work, thermal evaporation method has been allocated to deposit layers of thin film on commercial coated glass substrate, there was a thin layer of CdS of 50 nm thickness, followed by over layer of four sets of CdTe with different thickness ranging as 2, 4, 6, 8 μm to produce glass/CdS/CdTe layers of thin solar cells. The X-Ray Diffraction (XRD) and Scan Electron Microscopy (SEM) techniques have been used to study structural characterization. The UV-NIR Spectrophotometer equipment is to perform the optical characteristics of the prepared ~~solar~~ thin films.

2. Experiments:

CdS along with CdTe materials have been used to prepare thin films solar cells with a crystal purity of around 99.999%. Thermal evaporation method was used to deposit both CdTe and CdS layer. In this technique, CdS material was placed in a tungsten boat then evaporated on glass substrate and deposited with thickness of 50 nm. After that, all of the four films placed again in a chamber and deposited. The CdTe layer was deposited as set of different thicknesses of 2, 4, 6, 8 μm. The defined structure of the deposited layers was studied by using the ~~X-ray diffraction~~ (XRD) (Shimadzu 600,

Japan.). Morphology of the surface and Imaging of the microstructure analysis for the films at different deposition thicknesses was done using SEM model JEOL, operating at an accelerating voltage of 30kV. The transmission and absorption spectra of CdS/CdTe thin-film have been investigated using Spectrophotometer in the UV-NIR range from 300 to1100 nm.

3. Results and discussion

3.1 XRD characterization

Figure 1 shows the room temperature XRD spectra of CdS/CdTe films on glass substrate with thickness of 2 μm, 4 μm, 6 μm and 8 μm. The spectra shown in Figure 1 indicate that the films are polycrystalline in nature. Investigation of the XRD spectra of the of 2 μm films shows cubic zinc-blend type with cards number (JCPDS 80-0021 and 75-2085). In addition, three main XRD diffraction peaks are clearly detected for planes (111), (220) and (311) with preferred orientation along (111) plane at relative intensities 100%, 9% and 4%, respectively [1]. This result is in a good agreement with the results reported previously for CdS, CdTe and their compositions [2,3,4,6,7].

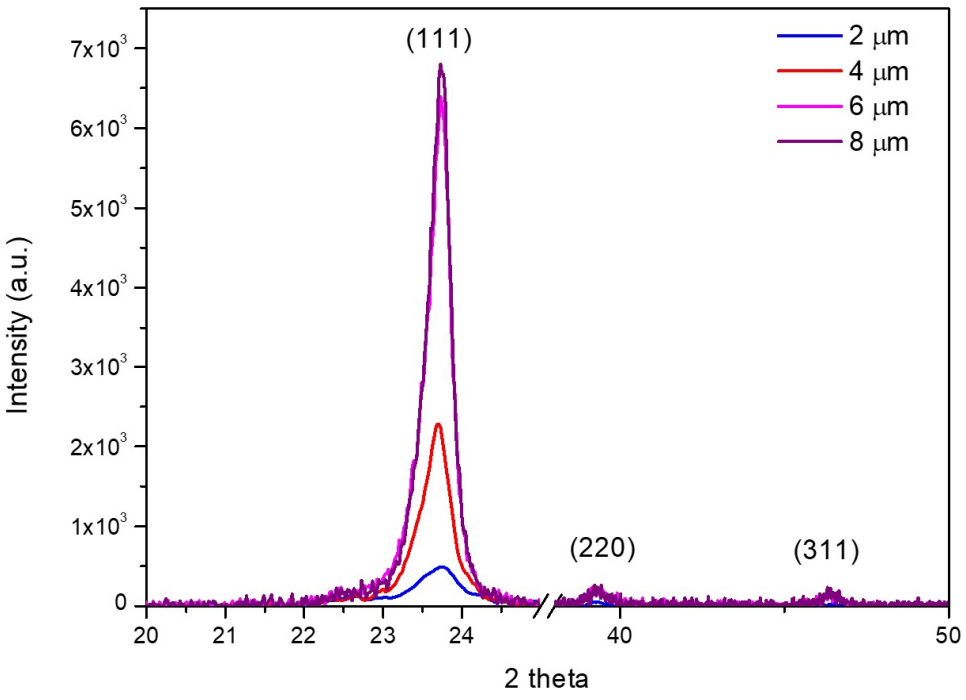

Figure 1 XRD spectra for nanocrystalline CdTe thin films with thickness as 2, 4, 6, and 8 μm**.**

Structural dependence of thickness for CdS/CdTe layers is also shown in Figure 1, where the peaks intensity increases with increasing thickness with almost the same main diffraction planes. However, the large intensity of the (111) diffraction peaks relative to the intensities of (220) and (311) peaks indicates preferential orientation of films in the (111) plane vertically to the substrate[11]. The full width at half maximum (FWHM) decreases noticeably with increasing thickness as clear in figure 2, which is associated with decreasing of the imperfection of the lattice that is resulted from interior macrostrain within atoms and subsequently allowing the increase of the crystallite size. The films dependence as a function of the thickness which is reported in this work also fits well with the similar studies reported for other materials [12, 16].

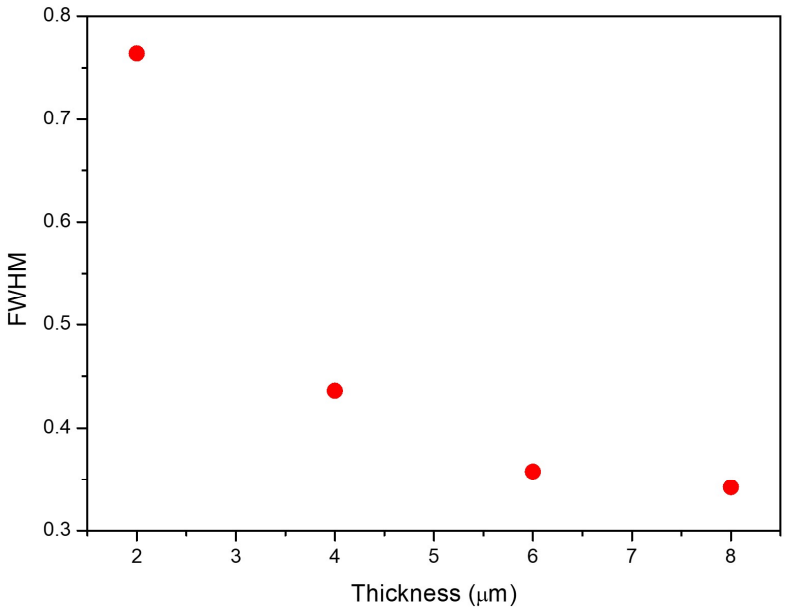

Figure 2 The FWHM as a function of the sample thicknesses (2, 4, 6, and 8 μm).

The lattice parameter (a) for the thin film unit cell for was calculated based on the equation below:

$$a=d\,(h^2+k^2+l^2)^{1/2} \qquad (1)$$

where d can be described as the interplanar spacing of the atomic planes, and (hkl) are Miller indices. It is been noticed that the lattice constant (a) is constant and not changing with changing thickness (t) for the prepared samples due to the fact that there is no change in the theta position or the material composition as the only parameter we have changed is the thickness. The value of the lattice constant

for all the thickness (2, 4, 6, and 8 μm) is found to be equal to 6.48 Å, where the FWHM is inverse with the thickness as shown in figure 2.

Table 1 The relation between the intensity and the thickness t (2, 4, 6, and 8 μm).

(hkl)	Intensity k/c/sec			
	t= 2	t= 4	t= 6	t= 8
(111)	493	5000	6330	6660
(200)	40.46	45.28	262	227
(311)	22.09	23	170	154

Average crystalline size (D) of CdTe layers is obtained from the FWHM for the three diffraction peaks using the following equation [18] :

$$D = \frac{k\lambda}{\beta_{2\theta}\cos\theta} \qquad (2)$$

This equation is called Scherrer equation, as k is the appreciation for Scherrer's constant (k) which is equal to 0.9, λ parameter is the XRD wavelength, which is equal to 1.54056Å, $\beta_{2\theta}$ is the FWHM representing the diffraction peak and θ constant is the Bragg diffraction angle. These results demonstrate that the size of crystallite is increasing from 13 nm at 2 μm to 30 nm at 8 μm. The micro-strain presented in the nanocrystalline thin films is due to the difference between the crystal size and the thickness, which can be estimated from the below equation:

$$\varepsilon = \frac{B\cos}{4} \qquad (3)$$

The calculated results indicated that the strain decreases from $3.98x10^{-3}(lin^{-2}.\ nm)$ at 2 μm to 8.98 $x10^{-3}$ $(lin^{-2}.\ nm)$ at 8 μm. For cubic structure of these samples, the dislocation density also been considered using the next equation [20]:

$$\delta = \frac{n}{D^2} \qquad (4)$$

where n is a factor which equals unity giving minimum dislocation density and D is the grain size. These results also indicates that the dislocation density decreases from 0.00529 nm^{-2} at 2 μm to 0.0010 nm^{-2} at 8 μm. The dislocation density is reduced according to equation 4 in consequence it is causing an increase in the crystal size, which indicates a lower number of lattice imperfections. This may be due to a decrease in the occurrence of grain boundaries because of an increase in the crystallite size of these films.

Figure 2 and table 1, 2 indicates that the FWHM decreases with increasing the film thickness which implies more crystalline attributed to the relaxation due to the little strain [20] with no effect on lattice parameters.

The variation in both micro strain and dislocation density with increasing layer thickness are due to the arrangement of Te atoms and being replaced by the Cd atoms which is related directly to the large atomic radius of Te (1.38Å), and Cd (1.44Å) compared to S (1.05Å).

Table 2 XRD parameters for the samples at different thickness (2, 4, 6, and 8 μm).

Samples	FWHM	D	micro strain	dislocation
2Micro	0.764	13.74	0.148158965	0.00529
4Micro	0.432	24.08	0.08377575	0.00174
6Micro	0.358	29.08	0.068281796	0.00128
8Micro	0.3418	30.46	0.065039364	0.0010

3.2 SEM characterization

SEM image is presented in figure 3. The sample surface studies suggests that the film is uniform, homogeneous and almost dense-packed with no voids, cracks or pinholes on the sample. All the four samples have the same uniform and homogeneous surface.

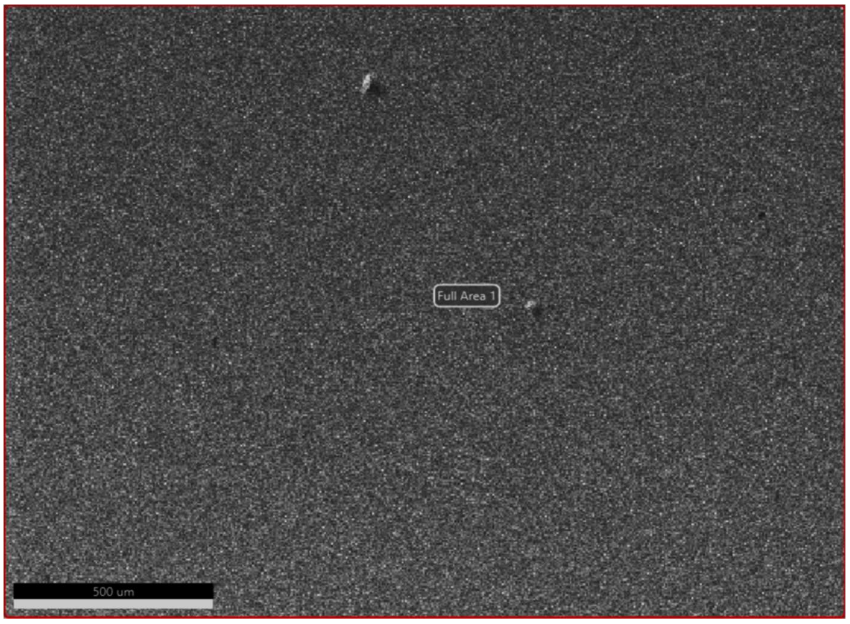

Figure 3 SEM image of CdS/CdTe thin films sample with thicknesses of (2μm).

3.3 Optical characterization

The optical properties of the samples (Absorbance A(λ), and reflectance R(λ)) have been investigated within the UV region from 350 nm to 800 nm. The results display the Absorbance A(λ), and reflectance R(λ) behaviours of a nanocrystalline thin film with changing the thickness (2, 4, 6, and 8 μm). Figure 4 represent increase in maximum intensity of the absorbance percentage with a clear shift from lower wavelength 354 nm to higher wavelength 414 nm of the absorption edge as the thickness increases from 2μm up to 8 μm. This red shift is related to the dependence of thickness and the optical energy band gap [21,22].

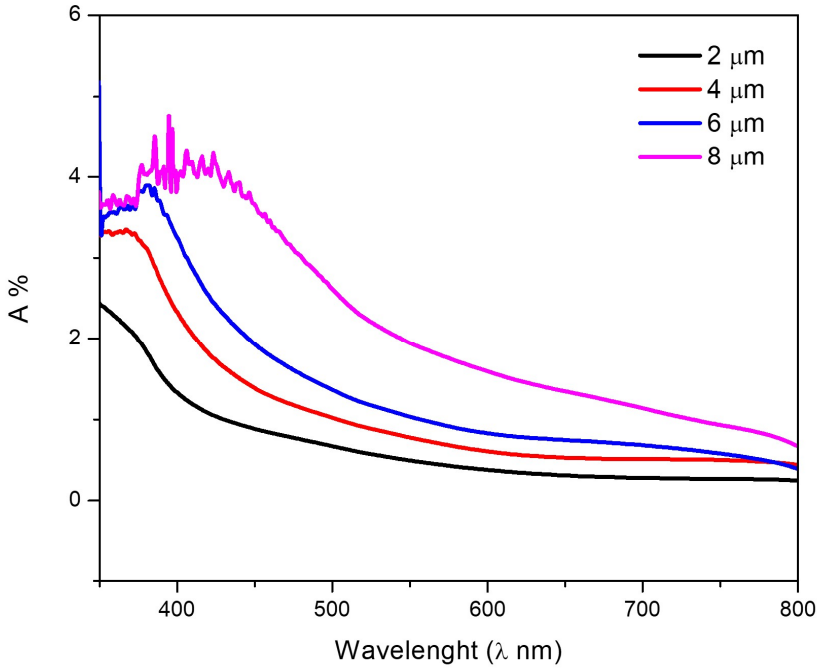

Figure 4 Spectral measurements of the Absorbance A(λ) of the samples measured at room temperature for thickness (2, 4, 6, and 8 μm).

Figure 5 illustrates an increase in the maximum intensity of the reflectance with a slight shift from lower wavelength 350 nm to higher wavelength 397.2 nm of the reflectance as the thickness increases from 2μm up to 8 μm. This red shift is associated with the dependence of thickness and the materials nature [23] the higher wave length mean lower energy reflected from thin-films that mean and indicate to higher energy absorbed and consequently lowering in optical energy gap.

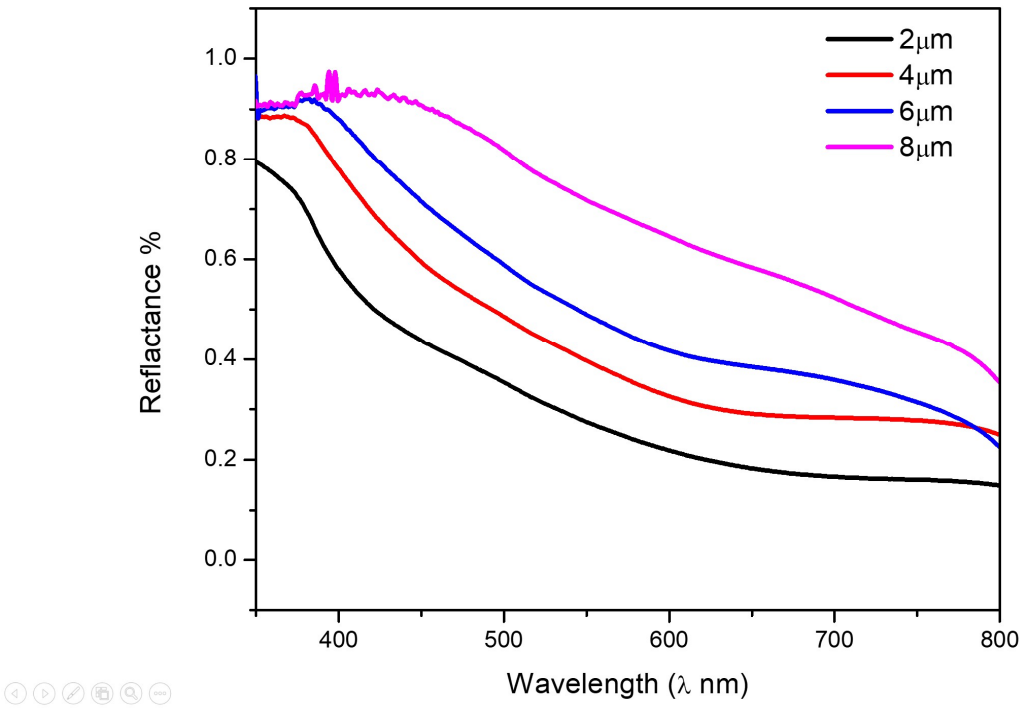

Figure 5 Spectral measurements of the reflectance R(λ) of samples measured at room temperature for thickness (2, 4, 6, and 8 μm).

2 The Absorption coefficient relationship:

The importance of calculating the optical absorption coefficient α for the thin films is to investigate the amount of absorbed light through these thin films, in particular within the strong absorption range, where the light intensity can be absorbed through.

Therefore, the Absorption coefficient is calculated experimentally from the next equation:

$$\boldsymbol{\alpha = \frac{2.303 * A}{t}} \qquad \textbf{(4)}$$

where A and t are the Absorption, and thickness respectively. The absorption essentially occurs as a result of the excitation process for the electron, were it transferred between the valance band and the conduction band. The energy gap of these spectra can be calculate using the following Tauc relation:

$$\alpha h\nu = \alpha_o (h\nu - E_g)^n \qquad \textbf{(5)}$$

Where Eg considered as the energy bandgap of the material, $\boldsymbol{\alpha o}$ is a constant parameter, α is an absorption coefficient, The photon energy is allocated by (hν) and (n) exponent which is identified optical transitions happened inside the materials. In figure 6 the red shift that occurs on the optical energy gap along with increasing the thickness is caused directly by high absorption of CdTe that have the energy bonds in the zincblende crystal structure for these materials. These observed bandgap data are in a good agreement with result [24].

The formation of additional defects during the deposion of the films can cause the decreases of energy band gap with increasing the thickness. Therefore, for thin films unsaturated bonds between atoms can result in lacking number of atoms. Accordingly, In thick film the unsaturated bonds results in increasing localized states width which placed in the band gap and allows a reduce of the energy band gap with thickness [25].

Table 3 Energy bandgap for samples at different thickness (2, 4, 6, and 8 μm).

Thickness (μm)	Energy gap (eV)
2	2.5
4	2.4
6	2
8	1.8

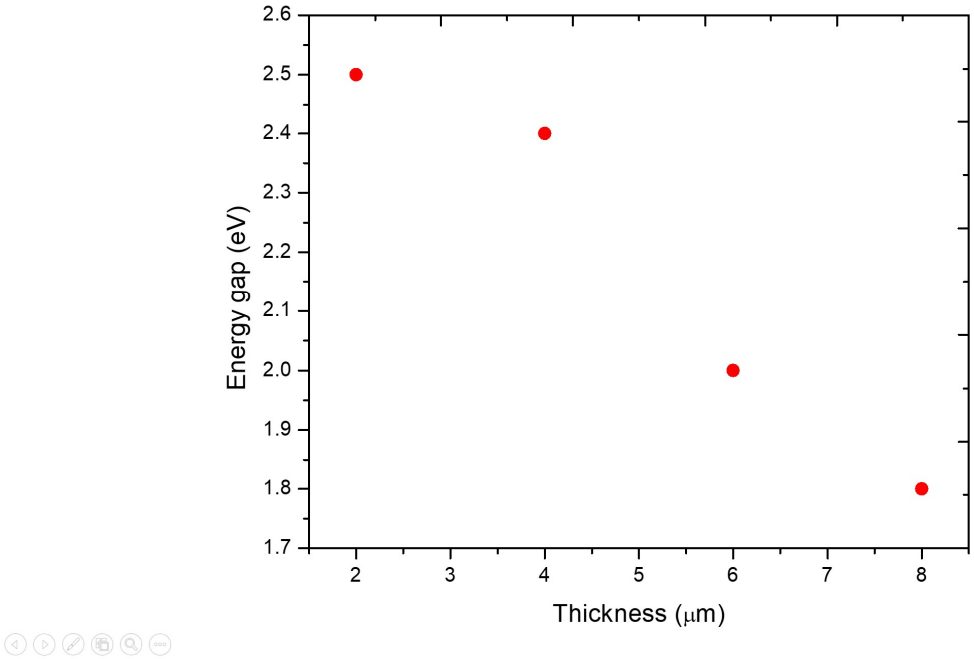

Figure 6 Optical energy band gap of the samples at different thickness (2, 4, 6, and 8 μm).

Conclusion:

In conclusion, we have demonstrated nanocrystalline hetero structure CdS/CdTe thin films which that been deposited on glass substrate using thermal evaporation method. XRD studies indicates that all the thin films have polycrystalline zinc blend crystal structure with a constant lattice parameter of 6.48 nm along with a decrease in the FWHM as the thicknesses increases from 2 μm to 8 μm. The average size of crystallite is increasing from 13 nm to 30 nm, also the strain increases from $3.98x10^{-3}(lin^{-2}.\ nm)$ to $8.98\ x10^{-3}\ (lin^{-2}.\ nm)$, and the dislocation density decreases from $5.293x10^{-4}(nm^{-2})$ to $1.0108x10^{-3}\ (nm^{-2})$ as the thicknesses increases from 2 μm to 8 μm respectively. The optical analysis reveals that there is a red shift from 354 nm to 414 nm of the absorption edge, with also a slight red shift from 350 nm to 397.2 nm of the reflectance edge as the thickness increases from 2μm up to 8 μm. Additionally, the band gap decreases from 2.5 to 1.8 eV with increasing the CdTe layer thickness.

References:

1.B. E. A. Saleh and M. C. Teich, ’Fundamentals of photonics’’, 2nd edition J. Wiley & Sons Ltd. 2007.

2. M. Emam-Ismail, M. El-Hagary, E.R. Shaaban, A.M. Al-Hedeib. "Microstructure and optical studies of electron beam evaporated ZnSe1−xTex nanocrystalline thin films", Journal of Alloys and Compounds, 2012

3. S. V. Gaponenko, Optical properties of semiconductor nanocrystals. 2nd edition published by Cambridge University Press, 1998.

4. S.Jana, e.a., Physica E, 39. 2007: p. P.109.

5. D. M. Meysing, M. O. Reese, C. W. Warren, A. Abbas, J. M.

6. D.W. Lane, Solar energy materials & Solar cells, 90. 2006.

7. J.H.e., Thin Solid Films 511-512. 2006: p. 443.

8. D. M. Meysing, M. O. Reese, H. P. Mahabaduge, W. K. Metzger, M. Burst, J. N. Duenow, T. M. Barnes and C. A. Woldena, Chemical and mechanical techniques enabling direct characterization of the CdS/CdTe heterojunction region in completed devices, IEEE., 1-6, 2015.

9. J. M. Kephart, R. Geisthardt and W. S. Sampath, Sputtered, oxygenated CdS window layers for higher current in CdS/CdTe thin-film solar cells, IEEE., 854–858, 2012.

10. Y. Sanchez, M. Espindola-Rodriguez, H. Xie, S. Lopez-Marino, M. Neuschitzer, S. Giraldo, M. Dimitrievska, M. Placidi, V. Izquierdo-Roca, F. A. Pulgarin-Agudelo, O. Vigil-Galan and E. Saucedo, Ultra-thin CdS for highly performing chalcogenides thin-film based solar cells, Sol. Energy Mater Sol. Cells., 158 (2), 138-146, 2016.

11. S. Sakka, ol-Gel Science and Technology processing characterization and application, published by academic kluwer. 2002.

12. P.R.N.e., J. Appl. Phys. 66. 1989: p. 4950.

13. K. Gea, J. Chena, B. Chena, Y. Shena, J. Guoa, F. Lib, H. Liua, Y. Xua and Y. Mai, Low work function intermetallic thin film as a back surface field material for hybrid solar cells, J. Sol. Energy., 162, 397-402, 2018.

14. G. Kartopu, D. Turkay, C. Ozcan, W. Hadibrata, P. Aurang, S. Yerci, H. E. Unalan, V. Barrioz, Y. Qu, L. Bowen, A. K. Gurlek, and S. J. C. Irvine, Photovoltaic performance of CdS/CdTe junctions on ZnO nanorod arrays, sol. energy mater sol. Cells., 176, 100-108, 2018.

15. J. Schaffner, M. Motzko, A. Tueschen, A. Swirschuk, H. J. Schimper, A. Klein, T. Modes, O. Zywitzki and W. Jaegermann, 12% efficient CdTe/CdS thin-film solar cells deposited by low-temperature close space sublimation, J. Appl. Phys., 110, 064508., 2011.

16. S. A. Mahmoud et. al, Applied surface science, 253. 2006: p. 2969.

17. W. J. Lee, J. Sharp, A. Gilberto, Umana-Membreno, J. Dell and L. Faraone, Deposition Heating Effect on CdS Thin Films Prepared by Thermal Evaporation for CdTe Solar Cells, IEEE., 153-155, 2014.

18. Nykyruy, L., et al., Evaluation of CdS/CdTe thin film solar cells: SCAPS thickness simulation and analysis of optical properties. Optical Materials, 2019. **92**: p. 319-329.

19. A. A. M. Farag, I. S. Yahia, T. Wojtowicz and G. Karczewski, Influence of temperature and illumination on the electrical properties of p-ZnTe/n-CdTe heterojunction grown by molecular beam Epitaxy, J. Phys. D: Appl. Phys., 43 (21), 215102, 2010.

20. Kumarasinghe, R., et al., A Comparative Study on CdS Film Formation under Variable and Steady Bath-Temperature Conditions. Semiconductors, 2020. **54**(8): p. 838-843.21.al., F.C.-B.e., Journal of Non-Crystalline Solids. 2008: p. 3756.

21. Hakeem, A.A., et al., Study the effect of type of substrates on the microstructure and optical properties of CdTe thin films. Optik, 2021. 225: p. 165390.

22. H. H. Ahmed and A. B. Dakhel, The Effect of the Solution Concentration on Structural and Optical Properties CdS Thin Films Prepared by Chemical Bath Deposition Technique,IJCRR., 4, 8-13, 2012.

23. H. A. Hussin, Preparation and Physical Characterization of CDS thin Films Deposited by Chemical Spray Pyrolysis, IJSRSET., 3(5), 321-323, 2017.

24. O. K. Echendu and I. M. Dharmadasa, Graded-Bandgap Solar Cells Using All-Electrodeposited ZnS, CdS and CdTe Thin Films, Energies., 8(5), 4416-4435, 2015.

25. K. M. M. Abo-Hassan et. al, Physica B, 358. 2005: p. 256.